milleCrepe: Extending Capabilities of Fluid-driven Interfaces with Multilayer Structures and Diverse Actuation Media

Qiuyu Lu
University of California, Berkeley
Berkeley, CA, USA
qiuyulu@me.com

Jifei Ou
MIT Media Lab
Cambridge, MA, USA
jifei@mit.edu

Lining Yao
University of California, Berkeley
Berkeley, CA, USA
liningy@berkeley.edu

Hiroshi Ishii
MIT Media Lab
Cambridge, MA, USA
ishii@media.mit.edu

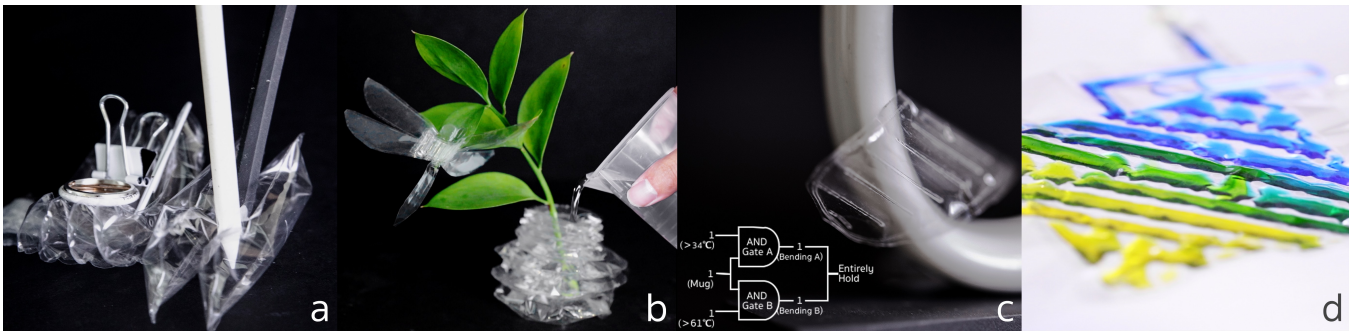

Figure 1: Example Applications of milleCrepe: (a) A desktop Organizer utilizing the dramatic volume change. (b) A watertight vase and a dragonfly decoration with shape-changing and stiffness-changing capabilities. (c) A responsive shape-changing mug mat with embedded logic structures for processing two input modalities non-electrically. (d) Stained glass with dynamic pattern changes.

ABSTRACT

This paper introduces milleCrepe, an innovative exploration of harnessing multilayer structures and diverse actuation mediums to expand the capabilities of the fluid-driven interface. Unlike prior pneumatic or hydraulic interfaces mainly focused on shape-changing output, milleCrepe may enable alternative deformation and more modalities through tuning multilayer chamber design and selecting appropriate actuation medium. For example, The collaboration of multilayer chambers results in a significant volume change, enabling the transformation of a 2D plane into a 3D solid. Selective actuation of different layers enables multiple shape changes. Furthermore, diverse actuation media inside different chamber layers can interact to create physical logic structures enabled by pressure difference, dynamic appearances corresponding to colored liquid mixtures, and tunable stiffness through phase changes. Additionally, several applications are presented to exemplify the potential of this technology in both product and interaction design.

Permission to make digital or hard copies of all or part of this work for personal or classroom use is granted without fee provided that copies are not made or distributed for profit or commercial advantage and that copies bear this notice and the full citation on the first page. Copyrights for third-party components of this work must be honored. For all other uses, contact the owner/author(s).
CHI EA '24, May 11–16, 2024, Honolulu, HI, USA
© 2024 Copyright held by the owner/author(s).
ACM ISBN 979-8-4007-0331-7/24/05
https://doi.org/10.1145/3613905.3650891

CCS CONCEPTS

• **Human-centered computing** → **Interactive systems and tools**.

KEYWORDS

Shape Change, Pneumatic, Hydraulic, Logic Structure, Fabrication

ACM Reference Format:
Qiuyu Lu, Jifei Ou, Lining Yao, and Hiroshi Ishii. 2024. milleCrepe: Extending Capabilities of Fluid-driven Interfaces with Multilayer Structures and Diverse Actuation Media. In *Extended Abstracts of the CHI Conference on Human Factors in Computing Systems (CHI EA '24), May 11–16, 2024, Honolulu, HI, USA.* ACM, New York, NY, USA, 10 pages. https://doi.org/10.1145/3613905.3650891

1 INTRODUCTION

Tangible user interfaces (TUIs) were once described as having limited ability to represent changes in material or physical properties, with it being challenging to change the form, position, or properties (e.g., color, size, stiffness) of physical objects in real-time [12, 20]. With the advent of new actuation technologies, shape-changing interface research has emerged and overcome these limitations to some extent [30]. However, while most works in this field focus on shape change, other output modalities such as color and stiffness have been relatively less explored, limiting the full potential of TUIs

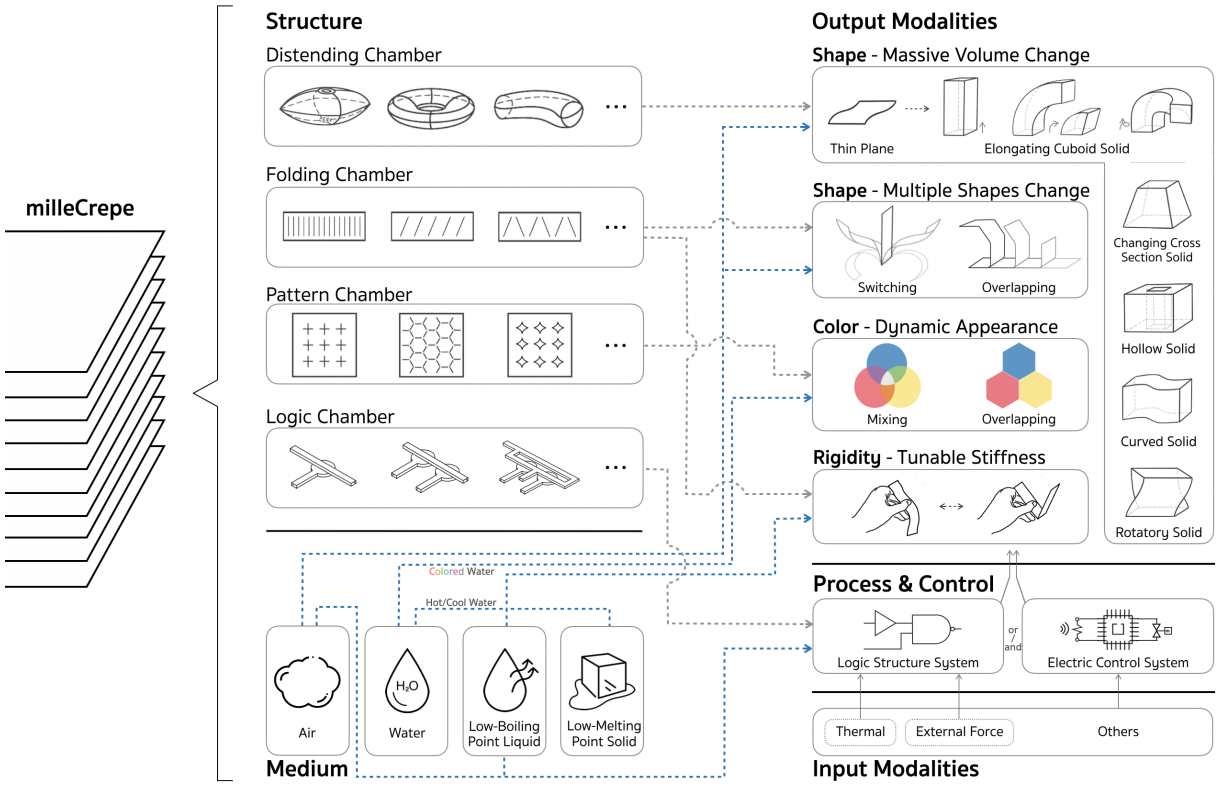

Figure 2: Design Space of milleCrepe.

[1]. As for the input, research has begun to investigate TUIs processing different input modalities through non-electrical physical or chemical mechanisms [28].

Made by combining multiple components with different properties, a composite material can have new properties that are superior to its individual constituents. In the field of soft robotics and fluid-driven interfaces (FDIs), a similar strategy has been taken to improve performance and enrich interaction. Materials like paper and fiber are embedded in an elastic substrate for tunning transformations [32, 40]. AeroMorph [25] has preliminarily explored quickly heat-sealing two layers of chambers which have different structures. Thus, the composite can switch between two shapes. AccordionFab [39] demonstrates an initial attempt to seal multiple plastic layers and limited shape-changing primitives are presented.

Inspired by these prior works, a question comes to mind: How far can we push such multilayer pneumatic composites? Evidently, we can customize the seam patterns of different layers and have them actuated selectively to achieve complex shapes. Besides this, looking at actuation mediums, they offer even more possibilities. Phase-changing mediums with high heat capacity counterparts allow stiffness changes. Colored mediums can alter appearance, and pressurizing mediums in different layers with varying pressure enables interactive dynamics, turning chambers into pneumatic valves or logic structures [22, 31]. This imparts on-board processing capabilities.

Employing the aforementioned strategy, we introduce milleCrepe, a multilayer-chamber composite for designing FDIs with enhanced capabilities. The multilayer-chamber structure facilitates the seamless integration of diverse chamber designs and various actuation mediums, enabling collaborative components to extend I/O modalities. In this paper, we delve into the design space of these composites, showcase primitives that exemplify their design and capabilities, and demonstrate motivating applications across various domains. We illustrate how different milleCrepe components can collaborate and interact, opening up new possibilities in interface design and enriching the library of FDIs.

2 RELATED WORK

Stemming from soft robotics, researchers in HCI have utilized fluidic actuation technologies to develop shape-changing interfaces. Notable examples include PneUI [40], Printflatables [33], PuPOP [35], AeroMorph [25], AccordionFab [39], Elliot W. Hawkes et al. [9], Pneuseries [3], and Sustainflatable [19], exploring various mechanisms and materials. Among them, aeroMorph [25] introduced a universal bending mechanism, investigating the use of two-chamber layers for shape change. AccordionFab [39] demonstrated laser-cut welding of multiple plastic layers, but it necessitates additional heat-resistant papers and has limitations in creating a few inflatable 3D objects. Additionally, alternative actuation mediums like low boiling-point liquid, UV-sensitive resin, water, and gas-generating chemicals have been investigated [8, 13, 16, 23, 37, 38].

Furthermore, in microfluidics, researchers have developed onboard logic structures using valves [22, 31]. This concept extends to robot design, with some studies utilizing advanced 3D printers for integrated fluidic circuits in a single print run [11, 38], and others employing silicone casting and assembly for modular fluidic computation structures [6, 27]. Rajappan et al. [29] demonstrated fluidic switches through heat-sealing textiles, building logic structures. However, these switches rely on large deformation of signal layer airbags under high pressure, causing disruptions in connected valves. Fluidic computation has gained attention in HCI [5, 34], but these designs use the beam reflection mechanism, limiting chainable structures, and are not widely adopted in microfluidics and robotics nowadays. The Fluidic Computation Kit offers modular building blocks for constructing complex fluidic computation units for FDIs, but block fabrication can be labor-intensive [18].

Despite recent research efforts, substantial potential remains in FDI. This research seeks to advance this field by exploring multilayer chamber structures using robotically sealed layers of thin thermal plastic film, eliminating the need for heat-resistant layers. In addition, our research focuses on how different layers of chambers and their actuation mediums can collaborate to enhance composite material properties, further expanding its capabilities.

3 MILLECREPE COMPOSITES OVERVIEW

The milleCrepe composites provide diverse design options (Fig. 2), incorporating four chamber structures and four mediums. These combinations yield interfaces with output modalities like volume change, shape variations, dynamic appearance, and tunable stiffness. An embedded logic structure offers a non-electrical control system, processing inputs such as thermal signals and external forces. Subsequent sections will detail milleCrepe's design space. The key to fabricating milleCrepe lies in controlling sealing parameters, particularly the press distance, to effectively seal only the top two layers of the film using a soldering iron. For more details regarding the fabrication method and material choice, please refer to the Appendix A.

3.1 Dramatic Volume Change

A single-layer chamber with pressurized distension has restricted expansion capabilities. However, the integration of multiple chambers enables substantial and customizable adjustments in volume. In Fig. 3.a, a primitive with four ~60 cm × 60 cm chambers, sealed with eight layers of 20 μm thick film and connected with circular air vents, transforms from a ~0.17 mm thin plane to a ~1000 mm tall solid upon inflation. While Prinflatables [33] briefly demonstrate a similar concept in their video, not elaborated in the paper, we delve into the implementation details of such a structure with our technology, offering enhanced control over its elongation. have Beyond straight line shapes, seam patterns can produce curved line shape transformations with controlled orientation. For instance, adding a line shape seam enables a sharp bend (Fig. 3.b). Dividing chambers in each layer into two different sizes achieves large radius bending (Fig. 3.c). Combining various seam designs creates a space curve (Fig. 3.d).

The seam patterns' design can be customized to enable transformations beyond a simple rectangular prism shape. In Fig. 4, four

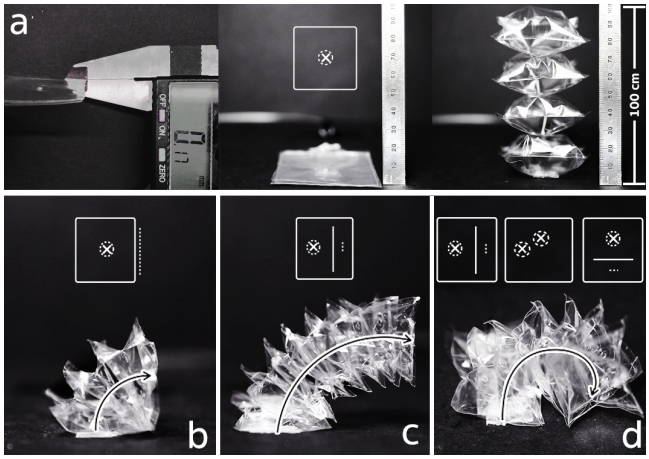

Figure 3: Examples of elongating cuboid solid. Unless otherwise stated, the solid lines/dotted lines/ "×" in the design patterns represent chamber seams/seams that bond adjacent chamber layers and seal the connecting vent/vent hole, respectively. (a) Linear transformation. (b-d) Curved transformation: Big curvature bending, Small curvature bending, and space curve.

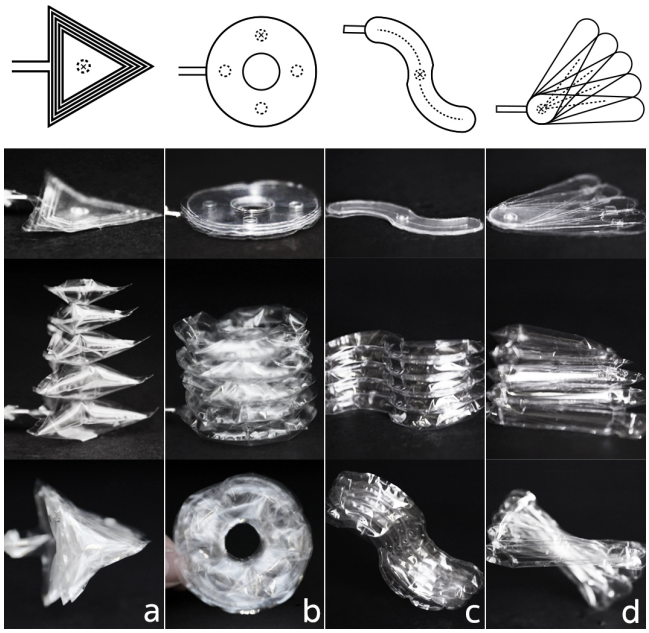

Figure 4: Examples of transformation from a thin plane to (a) Changing cross-section solid, (b) Hollow solid, (c) Curved solid, and (d) Rotatory solid.

examples showcase shapes achievable with different seam designs, including a changing cross-section, a hollow shape, a curved shape, and a rotatory shape. We have successfully created structures with up to 20 layers of film capable of a reversible change in volume. While theoretically, there is no limit to the number of layers that

can be stacked and sealed, increasing the layers may compromise the seal quality and reduce reversibility.

3.2 Multiple Shapes Change

When different folding chamber layers are stacked without connected via vents, independent actuation allows for switching among multiple shapes. In Fig. 5.a, a strip changes among three shapes. Simultaneously inflating multiple layers creates a combination of shapes (Fig. 5.b). It is crucial to pressurize the chamber layer furthest from the air inlet first, as closer layers' transformations may block the inlet air channel. The composite tends to bend toward the side with fewer film layers, providing control over the folding direction. Pressurizing a chamber layer can be hindered by films above and/or below, impacting deformation. For volume change primitives, adjacent chamber layers lack a shared film, and seam patterns only join

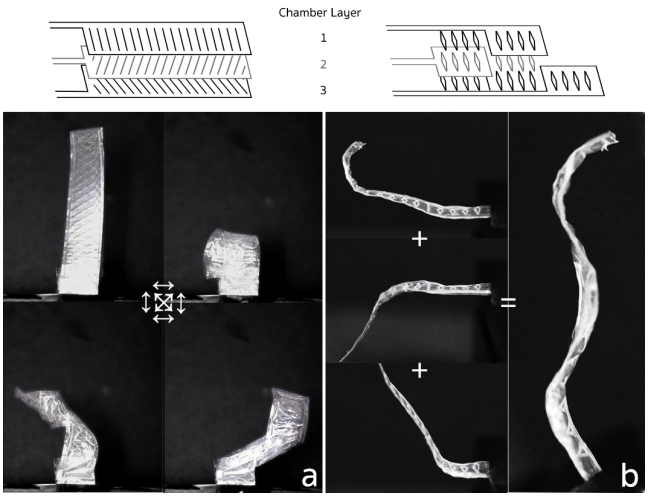

Figure 5: (a) A strip transform among multiple shapes. (b) Different chamber layers actuated together to combine into a new shape.

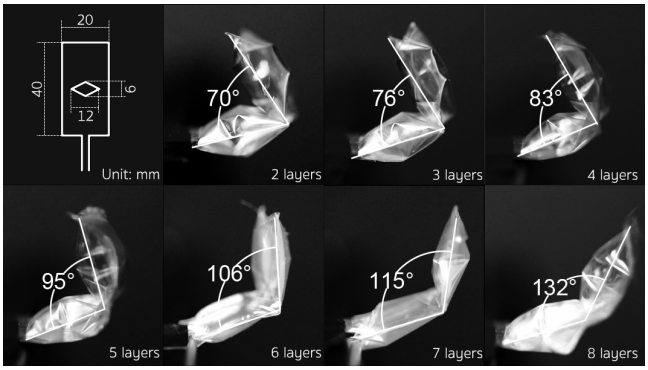

Figure 6: The number of film layers will affect the transforming performance of milleCrepe composites. The actuation pressure is 1.1 bar.

the layers and seal connecting air vents. In contrast, for multiple shape change primitives, a succeeding chamber layer can be created by directly sealing one film layer to the previous chamber, reducing the total number of films as adjacent layers share a common film. Fig. 6 illustrates how the performance of a standard bending unit, actuated under 1.1 bar, is affected by increasing the number of film layers. In practice, depending on seam complexity, a maximum of 3-4 chamber layers (4-5 film layers) can be sealed together while maintaining optimal multiple shape-transforming performance.

3.3 Dynamic Appearance

In Fig. 7, the left part of the primitive has three separate chamber layers filled with colored liquids, creating a pattern (Fig. 7.b). Liquids in the top and bottom layers flow to the middle layer through connecting vents on the right, resulting in the mixing of three colored liquids (Fig. 7.c). Constant inlet current yields laminar flows forming bar patterns, while inconsistent inlet current produces turbulent flows, generating ever-changing colors (Fig. 7.d). To prevent

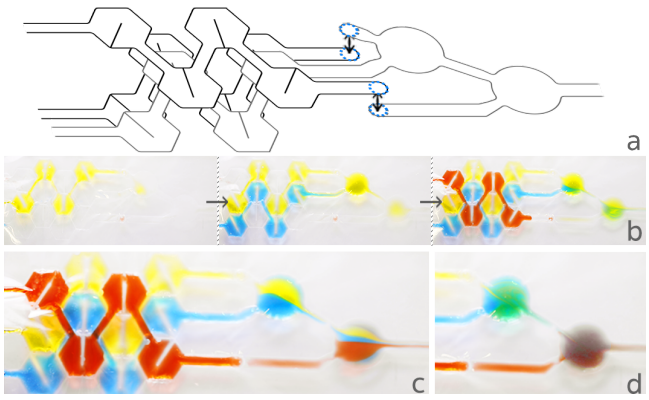

Figure 7: Dynamic Appearance Primitive: (a) The digital design of an appearance-changing primitive. Different chamber layers are connected at the blue dotted line circle. (b) Colored water is pumped into different layers respectively. (c) A laminar flow pattern forms in the right part of the sample with constant inlet flow. (d) A turbulent flow forms with inconsistent inlet flow. New colors are generated as the colored flows mix.

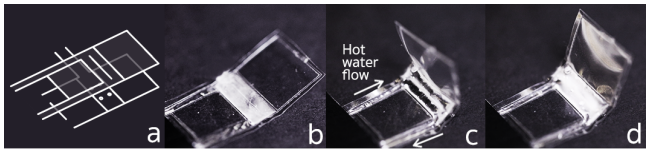

Figure 8: Tunable stiffness primitive: (a) The digital design of a tunable stiffness primitive. (b) The white part is the low temperature wax pre-injected into the bottom layer. (c) Hot water flow is pumped in and the wax melts. (d) The outlet is closed and the wax begins to solidify. The shape is then fixed.

channel blocking, the two layers of chambers do not share a middle film. In comparison to Venous Materials [21], which necessitates relatively specialized equipment for fabrication, our dynamic appearance primitives can be fabricated with greater accessibility. Additionally, our primitives can achieve heightened compliance as they are constructed from soft thin films.

3.4 Tunable Stiffness

Fig. 8 illustrates a bending primitive filled with low-temperature wax in the bottom chamber layer. Exposure to temperatures around 40°C softens the wax, and at 50°C, it completely melts. Injecting 60°C hot water into the top chamber layer causes the wax to soften, leading to the sample folding (Fig. 8.c). To maintain the folding shape, the outlet is closed as the water cools and the wax solidifies. After the wax becomes rigid, the water is removed, and the sample retains its folded shape (Fig. 8.d). This process is reversible, with hot water reintroduced to return to the original shape.

JamSheets [26] leverages the jamming phenomenon and vacuum to control stiffness, whereas our approach relies on phase-shift. Moreover, our methodology has the potential to enable non-electric shape and stiffness changes triggered by environmental stimuli. For example, a self-contained shape and stiffness change composite can be created by replacing hot water with pre-injected low-boiling point liquid, activated by an external heat source. When exposed to heat, the low boiling point liquid evaporates, inflating its chamber layer. As the wax in the other layer melts, the composite gradually deforms. Once the heat source is removed, the wax continues to release heat while solidifying, maintaining the inflation of the low-boiling-point liquid chamber layer until the wax hardens and fixes the shape.

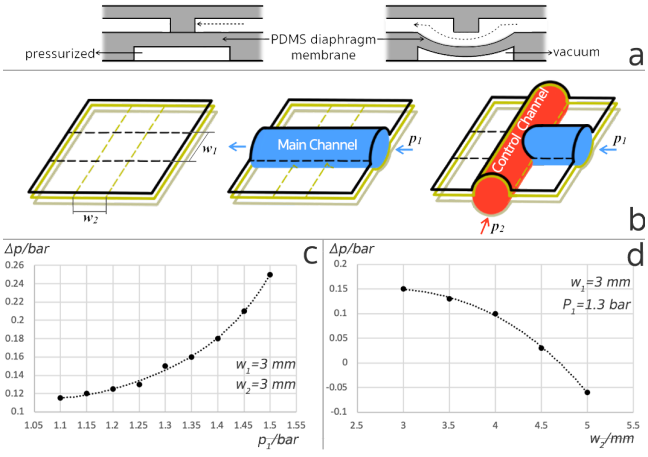

Figure 9: (a) The NOT gate mechanism in microfluidic chips. (b) The NOT gate mechanism in milleCrepe. (c) The correlation between the pressure in the main channel and the pressure difference needed when the main channel is blocked. (d) The correlation between the width of the control channel and the pressure difference needed when the main channel is blocked.

3.5 Embedded Logic Structure

The traditional NOT gate typically involves the deformation of a thin PDMS diaphragm membrane between two rigid substrates (Fig. 9.a). Alternatively, it can be made with thin and flexible films, requiring sophisticated techniques such as cold-pressing, molding/casting, or laser-micromachining for microscale channel creation [7]. The logic structure of milleCrepe operates differently from microfluidic chips. In Fig. 9.b, a NOT gate is created by sealing two channels that intersect vertically with three layers of film. When pressurized adequately, the medium fills the control channel, squeezing the top two layers of film tightly together to block the main channel. While this mechanism may not be as precise as microfluidic analysis, it is acceptable for "macro" interface design and is easier to fabricate.

To validate the efficacy of the technology, two experiments were conducted to assess the requisite pressure difference $\Delta p(p_2 - p_1$, where p_1/p_2 denotes the inlet pressure of the main/control channel) for activating a NOT gate. In the initial test, maintaining a fixed width of 3 mm for both the main channel (w_1) and control channel (w_2), Δp was measured under varying p_1. Figure 9.c illustrates that an elevated p_1 necessitates a higher Δp. Nonetheless, the gate generally requires minimal Δp for activation. In the second experiment, with w_1 and p_1 fixed at 3 mm and 1.3 bar respectively, Δp was measured under different w_2. Figure 9.d demonstrates that a larger w_2 corresponds to a lower Δp. Notably, when w_2 reaches 5 mm, the gate activates even when p_2 is lower than p_1. This is attributed to the wider channel being more easily inflated, resulting in higher force on the upper film due to the increased channel surface area. Both experiments were conducted under specific conditions: overall dimensions of 80 mm × 50 mm; 20 μm thick BOPP film; ~1 mm width of seam; air as the actuation medium; channels placed centrally; and the sample's four corners affixed to a rigid flat substrate.

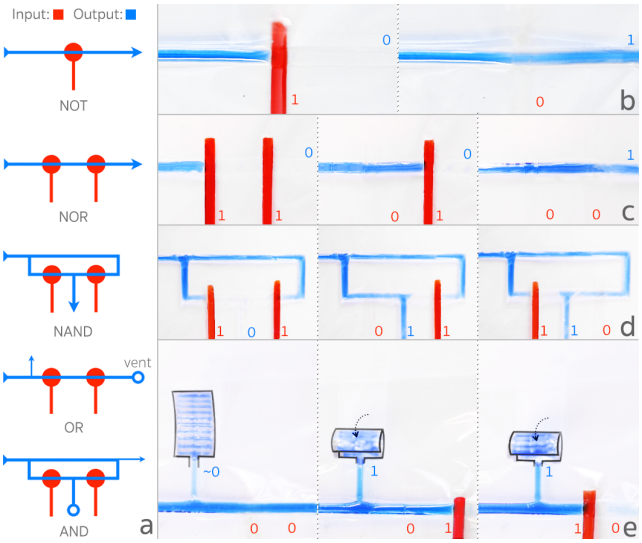

Figure 10: (a) The design of logic gates. (b) A NOT gate. (c) A NOR gate. (d)A NAND gate. (e)A OR gate. The AND gate will be demonstrated with an application example later.

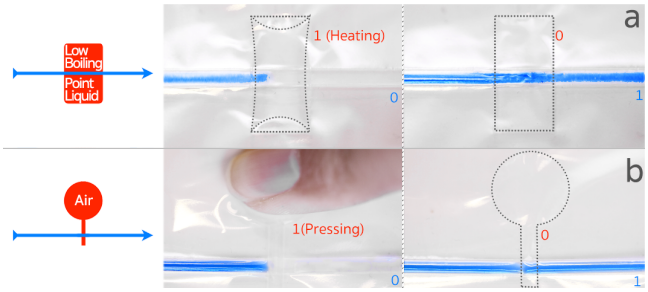

Figure 11: (a) A NOT gate activated by heat. (B) A NOT gate activated by external force.

Figure 10.b is an example of a NOT gate. Once we get a NOT gate, the NAND/NOR gate can be easily achieved by combining two NOT gates (Figure 10.c,d). However, the AND/OR gate will be a bit more complex. Figure 10.e shows a design of an OR gate. The output port branches from the main channel and it is half as wide as the main channel. When both inputs are "zero", the medium tends to flow along the main channel to the vent. The pressure is not high enough, and the bending unit connected to the output port will only slightly deform. Once any of the inputs turn to "one", the main channel will be blocked, and pressure will start to build up. Then, the bending unit can be fully actuated. The actual practice of AND gate will be demonstrated in an application example later. All examples in Figure 10 are demonstrated with colored water for better visual accessibility.

Furthermore, we investigated using physical processes to drive the gates and enable onboard multi-input sensing and processing. We present two NOT gate examples that respond to changes in temperature or external force. The first NOT gate (Fig. 11.a) utilizes a low boiling point liquid in the control chamber (Fig. 11.b). When heated, the chamber inflates and blocks the main channel. The second NOT gate has a control chamber with a small amount of air injected. When subjected to external force, the chamber's internal pressure increases and blocks the main channel.

4 APPLICATION EXAMPLES

Inflatable Appendix. The milleCrepe composites are exceptionally lightweight and thin, easily carried in a pocket, purse, or notebook (Fig. 12.a). Inflation and sealing are effortless using a clip or tape (Fig. 12.b, c). Fig. 12.d showcases a desk organizer with a concave area for small stationery and a pen-stand portion securely holding pens. Fig. 12.e presents a customizable vase with a watertight cavity formed by leaving the middle section of the bottom chamber layer uncut. The shape can be adjusted by altering seam patterns. Fig. 12.f features a dragonfly decoration that "ecloses" when exposed to hot water, with one chamber layer filled with Novec^{TM} 7000 and another with low-temperature wax. Fig. 12.g displays a flower-shaped base tightening around a rising rabbit toy, achieved by the central seam in the top film layers. All items can be deflated, stored, and reused.

Customized Air Pillow. Introducing an air pillow design that inflates all segments simultaneously, offering customization in length and orientation to optimize packaging space (Fig. 13). This customization improves filling efficiency compared to traditional air pillows. In an industrial setting, mass-customization can enhance packaging efficiency and product protection by precisely fitting the shape of each product.

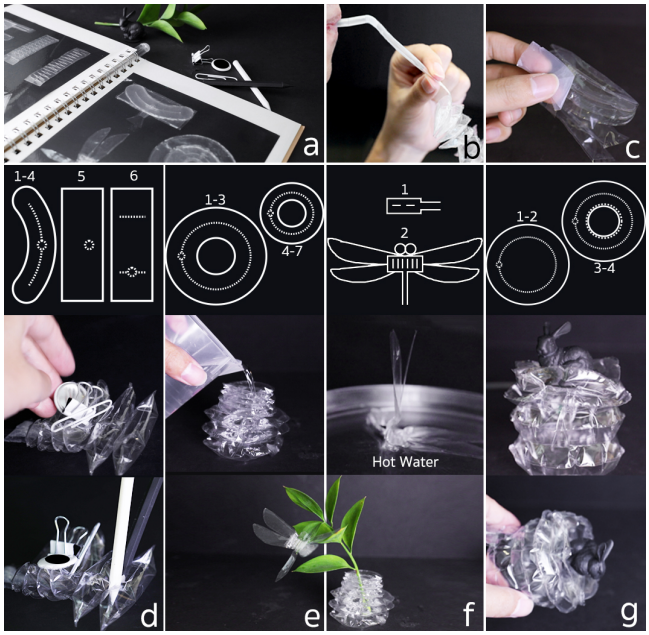

Figure 12: The inflatable appendix: (a) The milleCrepe composites are attached as the appendix of a notebook. (b, c) The attachments can be easily inflated and sealed. (d) A desk organizer. (e) A watertight vase. (f) A dragonfly decoration that will "eclose" when it touches hot water. (g) A flower shape base that will gradually clamp an object tightly with its petals when transforming.

Figure 13: Customized Air Pillow: (a) A customized L-shape air pillow (b) It ideally fills the entirety of the empty space within the packaging.

Responsive Mug Mat. To show the potential of the logic structure in enhancing I/O modalities, we created a shape-changing mat responsive to weight and heat inputs. The mug mat comprises three layers of chambers (Fig. 14.a, b). The bottom and top layers

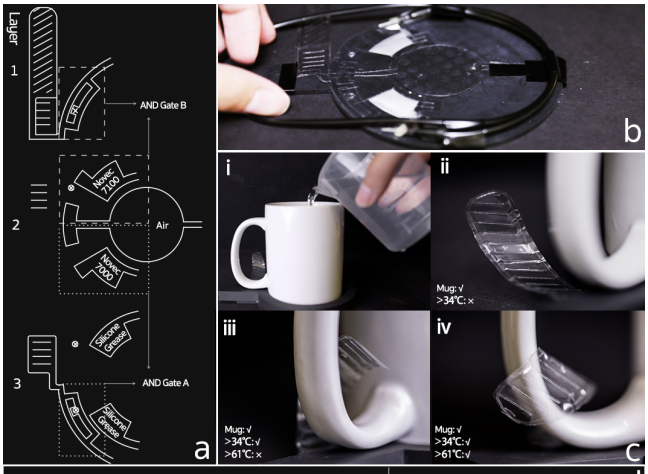

d

INPUT*			OUTPUT	
Mug	>34℃**	>61℃**	Bending A	Bending B
0	0	0	0	0
0	1	0	0	0
0	1	1	0	0
1	0	0	0	0
1	1	0	1	0
1	1	1	1	1

* Only conditions that can happen are listed. ** The boiling point of Novec™ fluid will rise as the pressure increases. The actual temperature when the channels get blocked will be slightly higher.

Figure 14: Responsive Mug Mat: (a) The digital design. (b) A closer view of the composites inside the mat. The white parts are heat-conducting silicone grease inside top layer chambers. (c) Different shape-changing outputs corresponding to different input conditions. (d) The truth table.

include bending actuators A and B, respectively, and main channels for AND gates A and B. The top layer also features two chambers filled with heat-conductive silicone grease to enhance thermal conductivity. The middle layer contains control channels, with a chamber containing Novec^{TM} 7000 for AND gate A, a chamber with Novec^{TM} 7100 (boiling-point 61°C) for AND gate B, and a chamber with pre-filled air for both AND gates.

When a mug is placed on the mat and hot water at ~80°C is poured in, the heat conducts through the mug to the mat (Fig. 14.c i, ii). Bending actuator A activates first, partially holding the handle (Fig. 14.c iii), followed by bending actuator B, which, combined with bending unit A, completely holds the handle (Fig. 14.c iv), signaling to the user that the mug is hot. As the water cools, bending actuator B deflates first, indicating that the water is warm and suitable for drinking. Then, bending actuator A reverses and fully releases the handle, indicating that the water is cold and ready for consumption if cold drinks are preferred. The logic is designed to make sure the bending units are activated only by the presence of a mug and cannot be triggered by environmental heat when no mug is on the mat. The complete truth table is presented in Fig. 14.d.

Dynamic Stained Glass. A thin milleCrepe composite, capable of color change, can be affixed to a window, transforming it into a dynamic stained glass. The prototype in Fig. 15 consists of

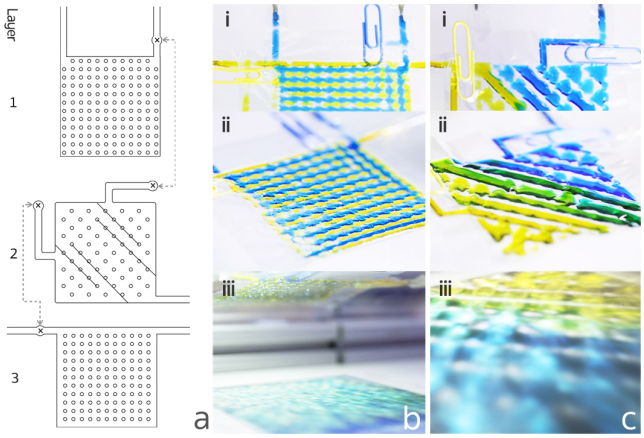

Figure 15: Dynamic Stained Glass: (a) The digital design. (b) A mosaic pattern on stained glass. (c)A gradient pattern on stained glass.

three chamber layers for creating patterns and two clips controlling colored water flow. With clips positioned as in Fig. 15.b i, yellow and blue water flows into the bottom and top layers, forming a mosaic pattern (Fig. 15.b ii). Clear water clears the chambers, and clips are repositioned for yellow and blue water to flow into the middle layer (Fig. 15.c i). Seams guide diagonal mixing, resulting in a vibrant color gradient pattern (Fig. 15.c ii). Both patterns cast beautiful shadows with mixed yellow, blue, and green colors (Fig. 15.b iii, c iii).

5 CONCLUSION AND FUTURE WORK

In this paper, we introduce MilleCrepe, a multilayer-chamber design strategy for extending the capabilities of FDIs. Our findings demonstrate how the different structures and mediums within the chamber layers of MilleCrepe can interact with each other, providing various types of I/O modalities transformations presented in previous work. These added features open new possibilities for interface design, applications, and expand the library of actuated thin film materials for HCI. However, there are limitations and areas for improvement, providing opportunities for future research and exploration. To facilitate the labor-intensive multiple layer seam patterns design, we can develop a Design Tool and providing a simulation function to streamline the iteration process [14, 42]. Further expansion of the design space, including introducing new structural designs and actuation mediums for detecting or outputting humidity level [41], magnetic fields [36], electric fields [15, 17], and weight [24], could enhance functionality. More evaluations, such as technical assessments (e.g., range of stiffness change), can deepen our understanding of performance, and user studies can shed light on how the extended functionalities improve the user experience.

ACKNOWLEDGMENTS

We appreciate Qiheqi Zhong for assisting with the sketches for Fig. 2. This work is partially supported by the National Science Foundation under Grant #2047912.

REFERENCES

[1] Jason Alexander, Anne Roudaut, Jürgen Steimle, Kasper Hornbæk, Miguel Bruns Alonso, Sean Follmer, and Timothy Merritt. 2018. Grand Challenges in Shape-Changing Interface Research. In *Proceedings of the 2018 CHI Conference on Human Factors in Computing Systems* (Montreal QC, Canada) *(CHI '18)*. Association for Computing Machinery, New York, NY, USA, Article 299, 14 pages.

[2] C Bonten and C Tüchert. 2002. Welding of Plastics-Introduction into Heating by Radiation. *Journal of reinforced plastics and composites* 21, 8 (2002), 699–709.

[3] Yu-Wen Chen, Wei-Ju Lin, Yi Chen, and Lung-Pan Cheng. 2021. PneuSeries: 3D Shape Forming with Modularized Serial-Connected Inflatables. In *The 34th Annual ACM Symposium on User Interface Software and Technology* (Virtual Event, USA) *(UIST '21)*. Association for Computing Machinery, New York, NY, USA, 431–440.

[4] Clearweld 2011. Clearweld coating products. http://www.clearweld.com/coatings-products.html.

[5] Jialin Deng, Patrick Olivier, Josh Andres, Kirsten Ellis, Ryan Wee, and Florian Floyd Mueller. 2022. Logic Bonbon: Exploring Food as Computational Artifact. In *CHI Conference on Human Factors in Computing Systems* (New Orleans, LA, USA) *(CHI '22)*. Association for Computing Machinery, New York, NY, USA, 1–21.

[6] Dylan Drotman, Saurabh Jadhav, David Sharp, Christian Chan, and Michael T. Tolley. 2021. Electronics-free pneumatic circuits for controlling soft-legged robots. *Science Robotics* 6, 51 (2021), eaay2627.

[7] Maximilian Focke, Dominique Kosse, Claas Müller, Holger Reinecke, Roland Zengerle, and Felix Von Stetten. 2010. Lab-on-a-Foil: microfluidics on thin and flexible films. *Lab on A Chip* 10 (2010).

[8] Juri Fujii, Satoshi Nakamaru, and Yasuaki Kakehi. 2021. Layerpump: Rapid prototyping of functional 3d objects with built-in electrohydrodynamics pumps based on layered plates. In *Proceedings of the Fifteenth International Conference on Tangible, Embedded, and Embodied Interaction* (Salzburg, Austria) *(TEI '21)*. Association for Computing Machinery, New York, NY, USA, 1–7.

[9] Elliot W. Hawkes, Laura H. Blumenschein, Joseph D. Greer, and Allison M. Okamura. 2017. A soft robot that navigates its environment through growth. *Science Robotics* 2, 8 (2017), eaan3028. https://doi.org/10.1126/scirobotics.aan3028 arXiv:https://www.science.org/doi/pdf/10.1126/scirobotics.aan3028

[10] Paul A Hilton, IA Jones, and Y Kennish. 2003. Transmission laser welding of plastics. In *First International Symposium on High-Power Laser Macroprocessing*, Vol. 4831. International Society for Optics and Photonics, 44–52.

[11] Joshua D Hubbard, Ruben Acevedo, Kristen M Edwards, Abdullah T Alsharhan, Ziteng Wen, Jennifer Landry, Kejin Wang, Saul Schaffer, and Ryan D Sochol. 2021. Fully 3D-printed soft robots with integrated fluidic circuitry. *Science Advances* 7, 29 (2021), eabe5257.

[12] Hiroshi Ishii, Dávid Lakatos, Leonardo Bonanni, and Jean-Baptiste Labrune. 2012. Radical Atoms: Beyond Tangible Bits, toward Transformable Materials. *Interactions* 19, 1 (Jan. 2012), 38–51.

[13] Shuguang Li, Daniel M Vogt, Daniela Rus, and Robert J Wood. 2017. Fluid-driven origami-inspired artificial muscles. *Proceedings of the National Academy of Sciences* 114, 50 (2017), 13132–13137. https://doi.org/10.1073/pnas.1713450114 arXiv:https://www.pnas.org/doi/pdf/10.1073/pnas.1713450114

[14] Qiuyu Lu, Yejun Liu, and Haipeng Mi. 2020. MotionFlow: Time-axis-based Multiple Robots Expressive Motion Programming. In *Proceedings of the 3rd International Conference on Computer Science and Software Engineering* (Beijing, China) *(CSSE '20)*. Association for Computing Machinery, New York, NY, USA, 145–149. https://doi.org/10.1145/3403746.3403919

[15] Qiuyu Lu, Chengpeng Mao, Liyuan Wang, and Haipeng Mi. 2016. LIME: LIquid MEtal Interfaces for Non-Rigid Interaction. In *Proceedings of the 29th Annual Symposium on User Interface Software and Technology* (Tokyo, Japan) *(UIST '16)*. Association for Computing Machinery, New York, NY, USA, 449–452. https://doi.org/10.1145/2984511.2984562

[16] Qiuyu Lu, Jifei Ou, João Wilbert, André Haben, Haipeng Mi, and Hiroshi Ishii. 2019. milliMorph – Fluid-Driven Thin Film Shape-Change Materials for Interaction Design. In *Proceedings of the 32nd Annual ACM Symposium on User Interface Software and Technology* (New Orleans, LA, USA) *(UIST '19)*. Association for Computing Machinery, New York, NY, USA, 663–672. https://doi.org/10.1145/3332165.3347956

[17] Qiuyu Lu, Danqing Shi, Yingqing Xu, and Haipeng Mi. 2020. MetaLife: Interactive Installation Based on Liquid Metal Deformable Interfaces. In *Extended Abstracts of the 2020 CHI Conference on Human Factors in Computing Systems* (Honolulu, HI, USA) *(CHI EA '20)*. Association for Computing Machinery, New York, NY, USA, 1–4. https://doi.org/10.1145/3334480.3383134

[18] Qiuyu Lu, Haiqing Xu, Yijie Guo, Joey Yu Wang, and Lining Yao. 2023. Fluidic Computation Kit: Towards Electronic-free Shape-changing Interfaces. In *Proceedings of the 2023 CHI Conference on Human Factors in Computing Systems* (Hamburg, Germany) *(CHI '23)*. Association for Computing Machinery, New York, NY, USA, Article 211, 21 pages. https://doi.org/10.1145/3544548.3580783

[19] Qiuyu Lu, Tianyu Yu, Semina Yi, Yuran Ding, Haipeng Mi, and Lining Yao. 2023. Sustainflatable: Harvesting, Storing and Utilizing Ambient Energy for Pneumatic Morphing Interfaces. In *Proceedings of the 36th Annual ACM Symposium on User Interface Software and Technology* (San Francisco, CA, USA) *(UIST '23)*. Association for Computing Machinery, New York, NY, USA, Article 32, 20 pages. https://doi.org/10.1145/3586183.3606721

[20] Haipeng Mi, Meng Wang, Qiuyu Lu, and Yingqing Xu. 2018. Tangible user interface: origins, development, and future trends. *SCIENTIA SINICA Informationis* 48, 4 (2018), 390–405. https://doi.org/10.1360/N112017-00227

[21] Hila Mor, Tianyu Yu, Ken Nakagaki, Benjamin Harvey Miller, Yichen Jia, and Hiroshi Ishii. 2020. Venous Materials: Towards Interactive Fluidic Mechanisms. In *Proceedings of the 2020 CHI Conference on Human Factors in Computing Systems* (Honolulu, HI, USA) *(CHI '20)*. Association for Computing Machinery, New York, NY, USA, 1–14.

[22] Bobak Mosadegh, Tommaso Bersano-Begey, Joong Yull Park, Mark A Burns, and Shuichi Takayama. 2011. Next-generation integrated microfluidic circuits. *Lab on a Chip* 11, 17 (2011), 2813–2818.

[23] Kenichi Nakahara, Koya Narumi, Ryuma Niiyama, and Yoshihiro Kawahara. 2017. Electric phase-change actuator with inkjet printed flexible circuit for printable and integrated robot prototyping. In *2017 IEEE International Conference on Robotics and Automation (ICRA)*. 1856–1863. https://doi.org/10.1109/ICRA.2017.7989217

[24] Ryuma Niiyama, Lining Yao, and Hiroshi Ishii. 2014. Weight and Volume Changing Device with Liquid Metal Transfer. In *Proceedings of the 8th International Conference on Tangible, Embedded and Embodied Interaction* (Munich, Germany) *(TEI '14)*. Association for Computing Machinery, New York, NY, USA, 49–52.

[25] Jifei Ou, Mélina Skouras, Nikolaos Vlavianos, Felix Heibeck, Chin-Yi Cheng, Jannik Peters, and Hiroshi Ishii. 2016. aeroMorph - Heat-sealing Inflatable Shape-change Materials for Interaction Design. In *Proceedings of the 29th Annual Symposium on User Interface Software and Technology* (Tokyo, Japan) *(UIST '16)*. ACM, New York, NY, USA, 121–132. https://doi.org/10.1145/2984511.2984520

[26] Jifei Ou, Lining Yao, Daniel Tauber, Jürgen Steimle, Ryuma Niiyama, and Hiroshi Ishii. 2014. jamSheets: thin interfaces with tunable stiffness enabled by layer jamming. In *Proceedings of the 8th International Conference on Tangible, Embedded and Embodied Interaction* (Munich, Germany) *(TEI '14)*. Association for Computing Machinery, New York, NY, USA, 65–72. https://doi.org/10.1145/2540930.2540971

[27] Daniel J Preston, Haihui Joy Jiang, Vanessa Sanchez, Philipp Rothemund, Jeff Rawson, Markus P Nemitz, Won-Kyu Lee, Zhigang Suo, Conor J Walsh, and George M Whitesides. 2019. A soft ring oscillator. *Science Robotics* 4, 31 (2019), eaaw5496.

[28] Isabel P. S. Qamar, Rainer Groh, David Holman, and Anne Roudaut. 2018. HCI Meets Material Science: A Literature Review of Morphing Materials for the Design of Shape-Changing Interfaces. In *Proceedings of the 2018 CHI Conference on Human Factors in Computing Systems* (Montreal QC, Canada) *(CHI '18)*. Association for Computing Machinery, New York, NY, USA, Article 374, 23 pages.

[29] Anoop Rajappan, Barclay Jumet, Rachel A Shveda, Colter J Decker, Zhen Liu, Te Faye Yap, Vanessa Sanchez, and Daniel J Preston. 2022. Logic-enabled textiles. *Proceedings of the National Academy of Sciences* 119, 35 (2022), e2202118119.

[30] Majken K. Rasmussen, Esben W. Pedersen, Marianne G. Petersen, and Kasper Hornbæk. 2012. Shape-Changing Interfaces: A Review of the Design Space and Open Research Questions. In *Proceedings of the SIGCHI Conference on Human Factors in Computing Systems* (Austin, Texas, USA) *(CHI '12)*. Association for Computing Machinery, New York, NY, USA, 735–744.

[31] Minsoung Rhee and Mark A Burns. 2009. Microfluidic pneumatic logic circuits and digital pneumatic microprocessors for integrated microfluidic systems. *Lab on a chip* 9, 21 (2009), 3131–3143.

[32] Daniela Rus and Michael T Tolley. 2015. Design, fabrication and control of soft robots. *Nature* 521, 7553 (2015), 467.

[33] Harpreet Sareen, Udayan Umapathi, Patrick Shin, Yasuaki Kakehi, Jifei Ou, Hiroshi Ishii, and Pattie Maes. 2017. Printflatables: Printing Human-Scale, Functional and Dynamic Inflatable Objects. In *Proceedings of the 2017 CHI Conference on Human Factors in Computing Systems* (Denver, Colorado, USA) *(CHI '17)*. ACM, New York, NY, USA, 3669–3680. https://doi.org/10.1145/3025453.3025898

[34] Valkyrie Savage, Carlos Tejada, Mengyu Zhong, Raf Ramakers, Daniel Ashbrook, and Hyunyoung Kim. 2022. AirLogic: Embedding Pneumatic Computation and I/O in 3D Models to Fabricate Electronics-Free Interactive Objects. In *Proceedings of the 35th Annual ACM Symposium on User Interface Software and Technology* (Bend, OR, USA) *(UIST '22)*. Association for Computing Machinery, New York, NY, USA, Article 9, 12 pages. https://doi.org/10.1145/3526113.3545642

[35] Shan-Yuan Teng, Tzu-Sheng Kuo, Chi Wang, Chi-huan Chiang, Da-Yuan Huang, Liwei Chan, and Bing-Yu Chen. 2018. PuPoP: Pop-up Prop on Palm for Virtual Reality *(UIST '18)*. Association for Computing Machinery, New York, NY, USA, 5–17. https://doi.org/10.1145/3242587.3242628

[36] Akira Wakita, Akito Nakano, and Nobuhiro Kobayashi. 2010. Programmable Blobs: A Rheologic Interface for Organic Shape Design. In *Proceedings of the Fifth International Conference on Tangible, Embedded, and Embodied Interaction* (Funchal, Portugal) *(TEI '11)*. Association for Computing Machinery, New York, NY, USA, 273–276.

[37] Penelope Webb, Valentina Sumini, Amos Golan, and Hiroshi Ishii. 2019. Auto-Inflatables: Chemical Inflation for Pop-Up Fabrication. In *Extended Abstracts of the 2019 CHI Conference on Human Factors in Computing Systems* (Glasgow, Scotland Uk) *(CHI EA '19)*. Association for Computing Machinery, New York, NY, USA, 1–6. https://doi.org/10.1145/3290607.3312860

[38] Michael Wehner, Ryan L Truby, Daniel J Fitzgerald, Bobak Mosadegh, George M Whitesides, Jennifer A Lewis, and Robert J Wood. 2016. An integrated design and fabrication strategy for entirely soft, autonomous robots. *Nature* 536, 7617 (2016), 451.

[39] Junichi Yamaoka, Kazunori Nozawa, Shion Asada, Ryuma Niiyama, Yoshihiro Kawahara, and Yasuaki Kakehi. 2018. AccordionFab: Fabricating Inflatable 3D Objects by Laser Cutting and Welding Multi-Layered Sheets. In *The 31st Annual ACM Symposium on User Interface Software and Technology Adjunct Proceedings* (Berlin, Germany) *(UIST '18 Adjunct)*. Association for Computing Machinery, New York, NY, USA, 160–162.

[40] Lining Yao, Ryuma Niiyama, Jifei Ou, Sean Follmer, Clark Della Silva, and Hiroshi Ishii. 2013. PneUI: Pneumatically Actuated Soft Composite Materials for Shape Changing Interfaces. In *Proceedings of the 26th Annual ACM Symposium on User Interface Software and Technology* (St. Andrews, Scotland, United Kingdom) *(UIST '13)*. ACM, New York, NY, USA, 13–22. https://doi.org/10.1145/2501988.2502037

[41] Lining Yao, Jifei Ou, Chin-Yi Cheng, Helene Steiner, Wen Wang, Guanyun Wang, and Hiroshi Ishii. 2015. BioLogic: natto cells as nanoactuators for shape changing interfaces. In *Proceedings of the 33rd Annual ACM Conference on Human Factors in Computing Systems*. ACM, 1–10.

[42] Tianyu Yu, Mengjia Niu, Haipeng Mi, and Qiuyu Lu. 2024. MilliWare: Parametric Modeling and Simulation of Millifluidic Shape-changing Interface. In *Proceedings of the Eleventh International Symposium of Chinese CHI* (Denpasar, Bali, Indonesia) *(CHCHI '23)*. Association for Computing Machinery, New York, NY, USA, 461–467. https://doi.org/10.1145/3629606.3629654

A FABRICATION PROCESS

The fabrication platform and process are similar to those proposed in [16, 25]. For researchers and designers interested in experimenting with the multilayer milleCrepe we introduced, additional details are provided in this appendix.

A.1 Material Selection

Fabricating multilayer heat-sealed structures requires PET or BOPP films with double-sided heat-sealable coatings. The 20 μm thickness of the film, even when stacked in multiple layers, enhances shape-changing performance compared to thicker materials. This thin film provides improved transmittance and faster heat conduction, making it ideal for applications requiring dynamic appearance or tunable stiffness. In summary, double-sided heat-sealable thin-film material is optimal for creating efficient multilayer heat-sealed chamber structures.

	Contact Sealing	Non-contact Sealing		
	Soldering Iron	Hot Air	Infrared LED	Infrared Laser
Sealing Speed	High	High	Low	Very High
Submillimeter Fabrication	Difficult	Yes	Difficult	Yes
Surface Damage	Happens	No	No	No
Surface Smoothness	Acceptable	Good	Good*	Good
Surface Precoat	No	No	Required	Required
Over Weld of Lower layers	Happens Occasionally	Infrequent	Infrequent	Infrequent
Z-axis Reorientation	Every layer	Not Necessary	Not Necessary	Not Necessary
Equipment Cost	Every Low	Low	Low	High
Simultaneous Multilayer Sealing	No	No	Yes	Yes
Film Color	No Limit	No Limit	Must Be Infrared Transmitting	

* When using high thermal shrinkage film, shrink and rugged surface may occur.

Figure 16: Comparison of different fabrication methods for multilayer heat sealing. Tested with 20 μm BOPP film.

A.2 Digital Design

To enhance the sealing process quality, consider the following guidelines for designing seam patterns:

- Fillet corners to prevent over welding, especially at small angled corners where the CNC platform may slow down, leading to increased heat accumulation.
- Insert breaking points along long seams and periodically lift the heating tool away to avoid surface wrinkles. Continuous pressure can cause friction, resulting in wrinkles perpendicular to the tool-path.
- When using infrared sealing, stagger overlapping seam patterns on different layers slightly to facilitate simultaneous multilayer sealing.

A.3 Robotic Heat Sealing

We compared several heat-sealing methods from various perspectives (Fig. 16). HCI researchers and designers can choose the most suitable method based on their situation.

A.3.1 Soldering Iron Sealing. By controlling sealing parameters, such as press distance, we can effectively seal only the top two layers of BOPP film using a soldering iron (Fig. 17.a). For 20 μm thick BOPP film, the optimal press distance is three to four times the film thickness, and the sealing temperature should be set at 200°C with a sealing speed of 500 mm/min. To ensure a constant press distance, it is necessary to reorient the z-axis for each layer. As the sealing tool's tip becomes smaller, the risk of surface damage, such as scratches and penetration, increases, especially when the tip diameter is below 1 mm. During the sealing process, the movement

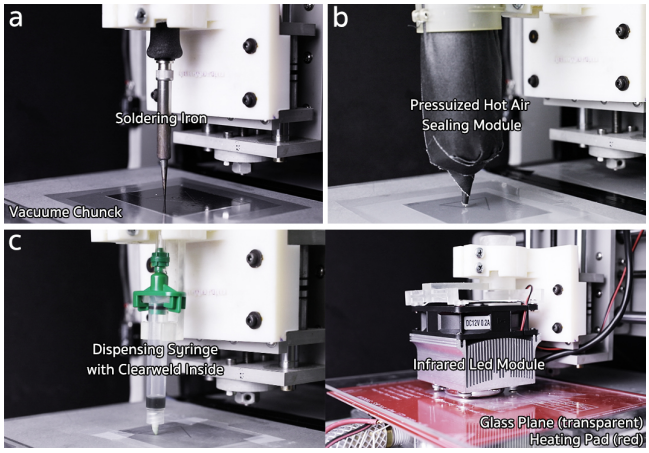

Figure 17: (a) Contact soldering iron sealing. (b) Non-contact hot air sealing. (c) Non-contact infrared based sealing (right) and ancillary infrared-absorbing solution coating (left) system.

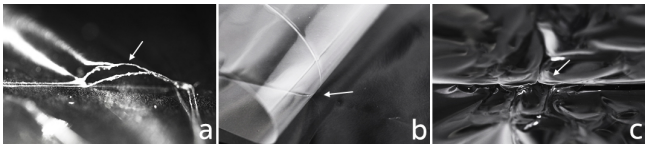

Figure 18: Examples of sealing failures. (a) Surface fold and penetration with soldering iron sealing. (b) Pseudo soldering with hot air sealing. (c) Heat shrinkage with infrared LED sealing

of the sealing tool press may cause surface wrinkles, which can accumulate as the film stacks, increasing the likelihood of sealing failure on subsequent layers (Fig. 18.a). However, this is rarely a concern with the first few layers. The contact sealing tool results in a concave seam with a raised edge. If seams of different layers intersect, there may be over-welding on the raised edges, leading to weak joints that can easily be separated when the composites are inflated.

A.3.2 Hot Air Sealing. We tested the pressurized hot air sealing method proposed by [16], suitable for thin-film sealing (Fig. 17.b). With a sealing speed of 300mm/min, air temperature at 200°C, and air pressure at 2 bar for 20 μm thick BOPP film, it showed smooth welding seams and minimal failures. Preheating the air barrels is crucial to avoid pseudo soldering (Fig. 18.b). Compared to contact sealing, hot air sealing results in fewer failures, smooth seams, and no surface damage or wrinkles.

A.3.3 Infrared Sealing. The use of CO_2 and infrared lasers for plastic parts cutting and welding is common in industry [2, 10]. Infrared laser welding is suitable for thin-film sealing, and a glass panel can be applied for pressure. Transparent plastic film needs coating with an infrared-absorbing solution like Clearweld® LD920F [4]. We used a Nordson Ultimus V dispenser with a custom syringe tip for application (Fig. 17.c left). Regular needle tips are not suitable due to solvent leakage. As access to infrared laser machines can be challenging, we propose a cost-effective alternative using a 25 mm × 25 mm, 100 W, 940 nm infrared LED (Fig. 17.c right). The LED module descends, presses a glass panel against the film for around 90 seconds, then lifts and moves to the next area. A heating pad has been added for efficiency. Preheating it to around 60°C reduces sealing time by at least half. Infrared sealing can simultaneously weld multiple film layers, demonstrated successfully with four layers. However, it may not be ideal for materials with high thermal shrinkage, causing overheating and shrinking (Fig. 18.c). Infrared LED sealing is less efficient but can be a good choice with access to an infrared laser machine.

A.4 Cutting, Punching & Closing Seal

If all seam patterns share the same exterior outline, the milleCrepe composites can be cut using a drag knife. However, for different patterns, films should be processed with a cutting plotter before sealing. It's advisable to place smaller seam patterns in lower layers for easier clamping by the vacuum chuck. For connecting adjacent chamber layers, punching is necessary. For a single connecting hole, manual creation through heat penetration is possible. Multiple holes require a cutting plotter. Positioning marks should be left on the first film layer and all others cut by the plotter. Finally, connect the composites to an external tube and seal with glue.